Assembly duration, cooling kinetics and textural maturation of a small-sized granite pluton

Nicolas Esteves[1*] ; Lydéric France[1,2] ; Catherine Annen[3] ; Pierre Bouilhol[1] ; Marian B. Holness[4]

[1] Université de Lorraine, CNRS, CRPG, 54000 Nancy, France

[2] Institut Universitaire de France (IUF), France

[3] Institute of Geophysics of the CAS, Prague 4, Czech Republic

[4] Department of Earth Sciences, University of Cambridge, Downing Street, Cambridge CB2 3EQ, United Kingdom

*Corresponding author: nicolas.esteves@univ-lorraine.fr

<u>List of appendices in this supplementary document:</u>

Supplementary figure A1: Relationship between the Beauvoir magma temperature and its crystal fraction used in this study, and determined from the crystallisation experiments of *Pichavant (2022)* with Beauvoir material (U_4d) as starting material. Note the that the magma-mush transition (crystal fraction: 50%) corresponds to a magma temperature of 575°C. Also note the greater crystallisation rate at lower temperature compared to that at higher temperature.

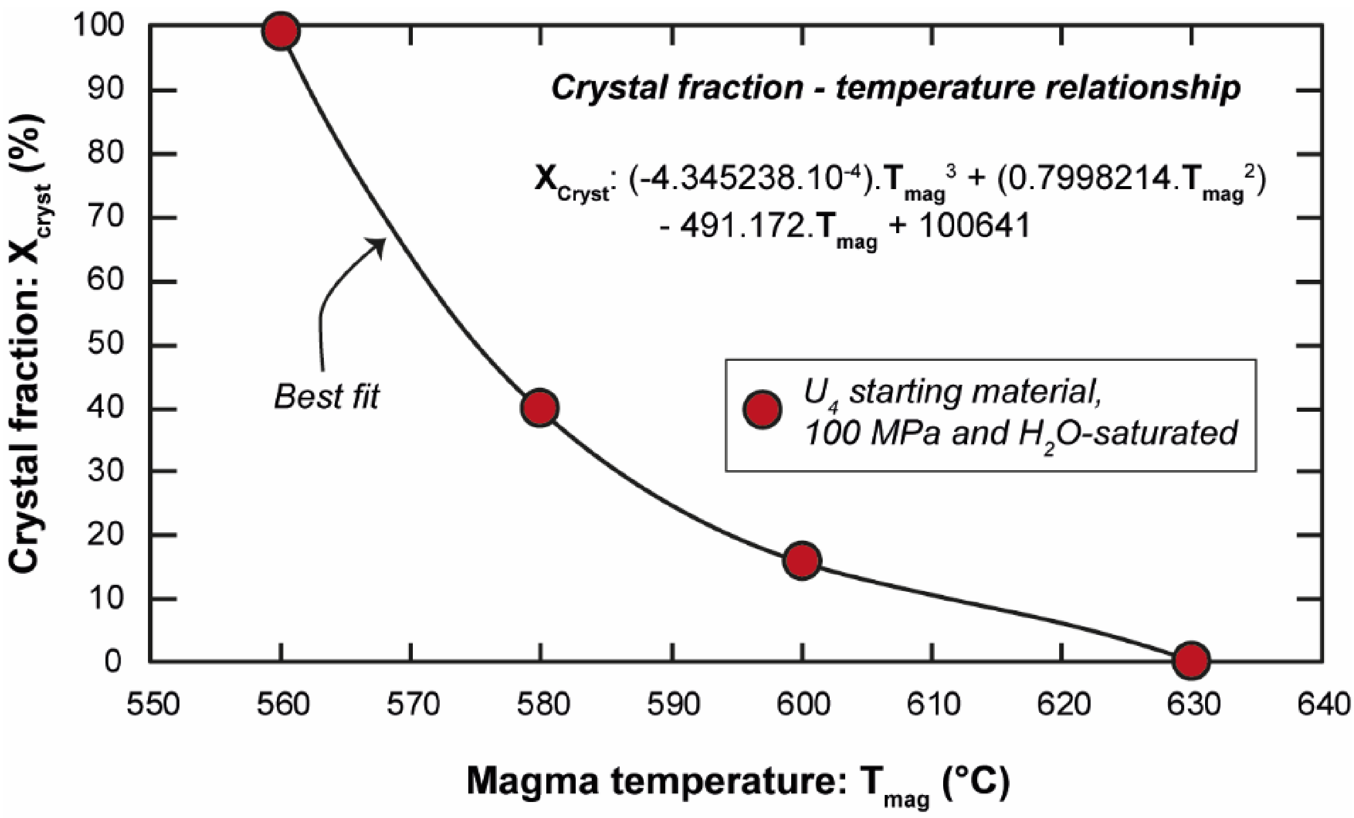

Supplementary figure A2: Temperature profil during the Beauvoir granite construction and solidification between 2,200 and 3,500 m obtained when each sill intrudes once the system is fully solidified (T_{crit} = 560°C). Note the downward progressive Beauvoir construction through time due to the general sill over-accretion. Numbers in boxes corresponding to each intruded sill according to their intrusive sequence. The simplified log on the right (based on Fig. 1a; *Esteves et al., 2025*) indicates the location of each sill at the end of the Beauvoir construction. Note the increase of the magma and mush fraction directly after a sill injection, indicating the host partial re-melting.

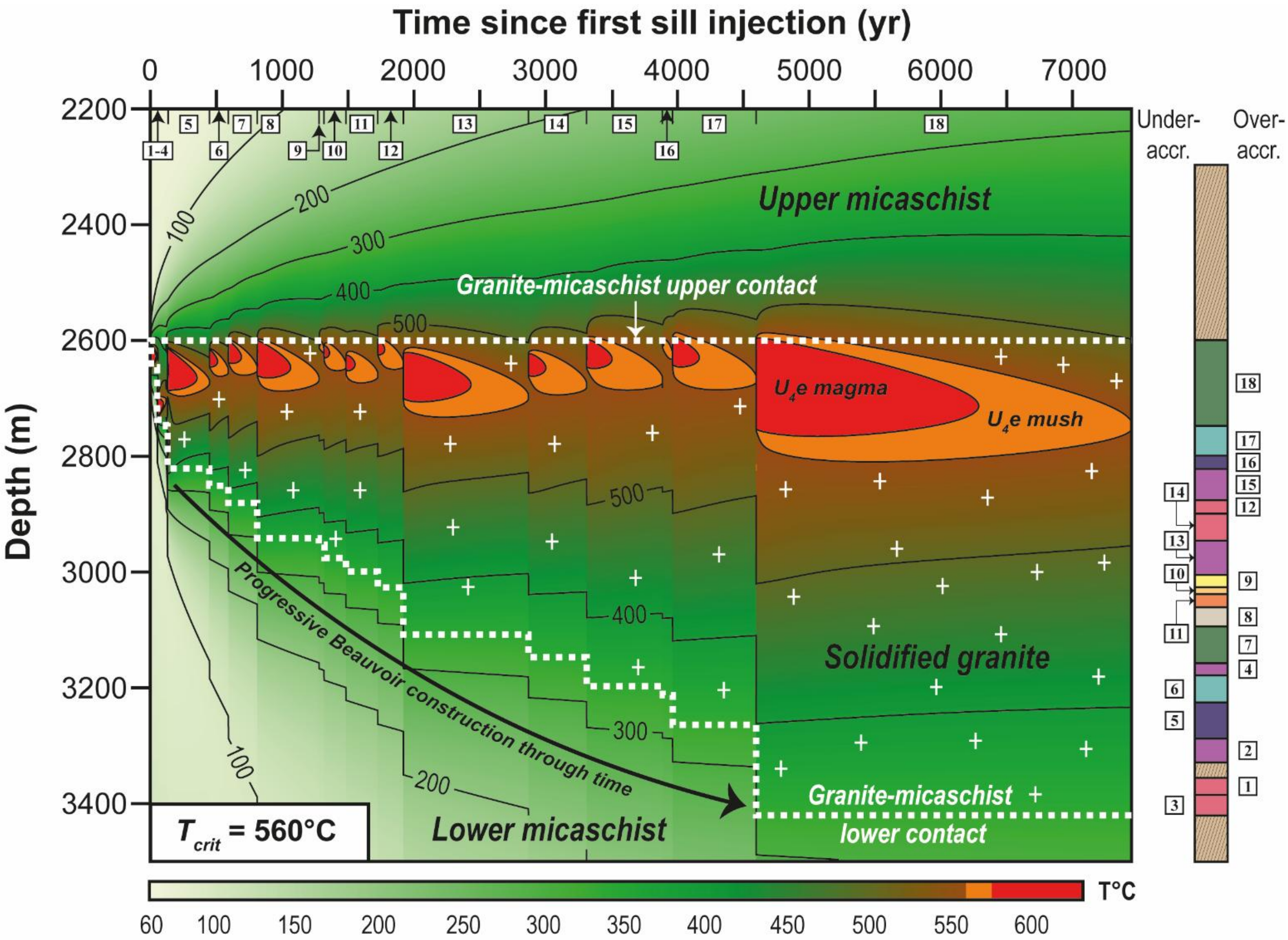

Supplementary figure A3: Temperature profil during the Beauvoir granite construction and solidification between 2,200 and 3,500 m obtained when each sill intrudes once the system is fully solidified and below 425°C (T_{crit} = 425°C). This temperature corresponds to the maximum temperature limit at which sharp contacts are preserved between each injected sill. Note the downward progressive Beauvoir construction through time due to the general sill over-accretion. Numbers in boxes corresponding to each intruded sill according to their intrusive seqeunce. The simplified log on the right (based on Fig. 1a; *Esteves et al., 2025*) indicates the location of each sill at the end of the Beauvoir construction. Note the progressive decrease of both the magma and mush fractions through time after a sill injection indicating that the host is not re-melting.

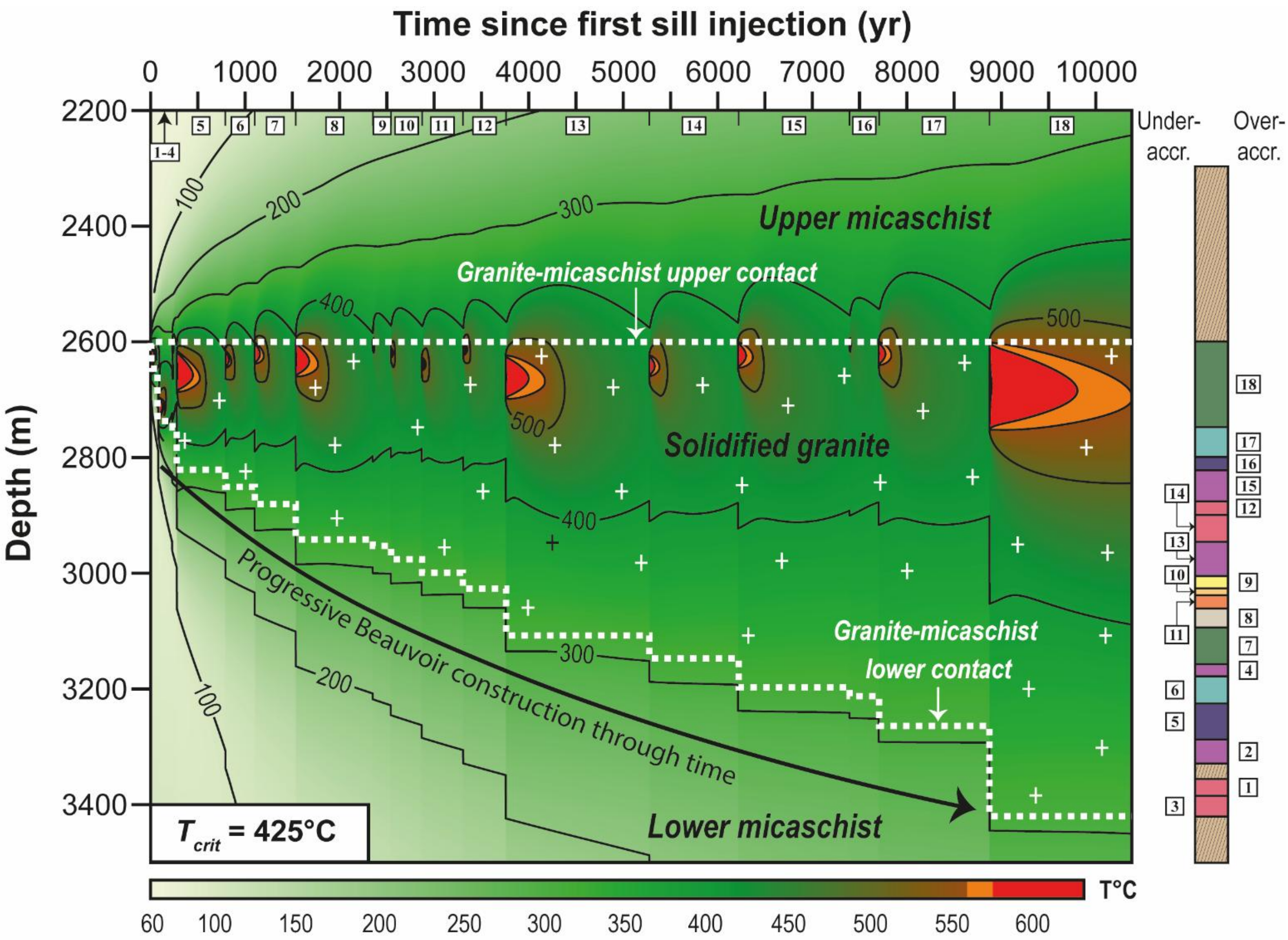

Supplementary figure A4: Temperature profil during the Beauvoir granite construction, solidification and progressive cooling over 100,000 years between the surface (0 m) and 7,000 m obtained when each sill intruded a mushy or fully solidified granite (T_{crit} = 575°C). This temperature corresponds to the magma-mush transition of Beauvoir magmas. Note that after 100,000 yr, the thermal anomaly induced by the Beauvoir granite emplacement is still present (i.e., 200 °C at 3,700 m). Also note that after ~30,000 yr, the whole granite is below 300 °C.

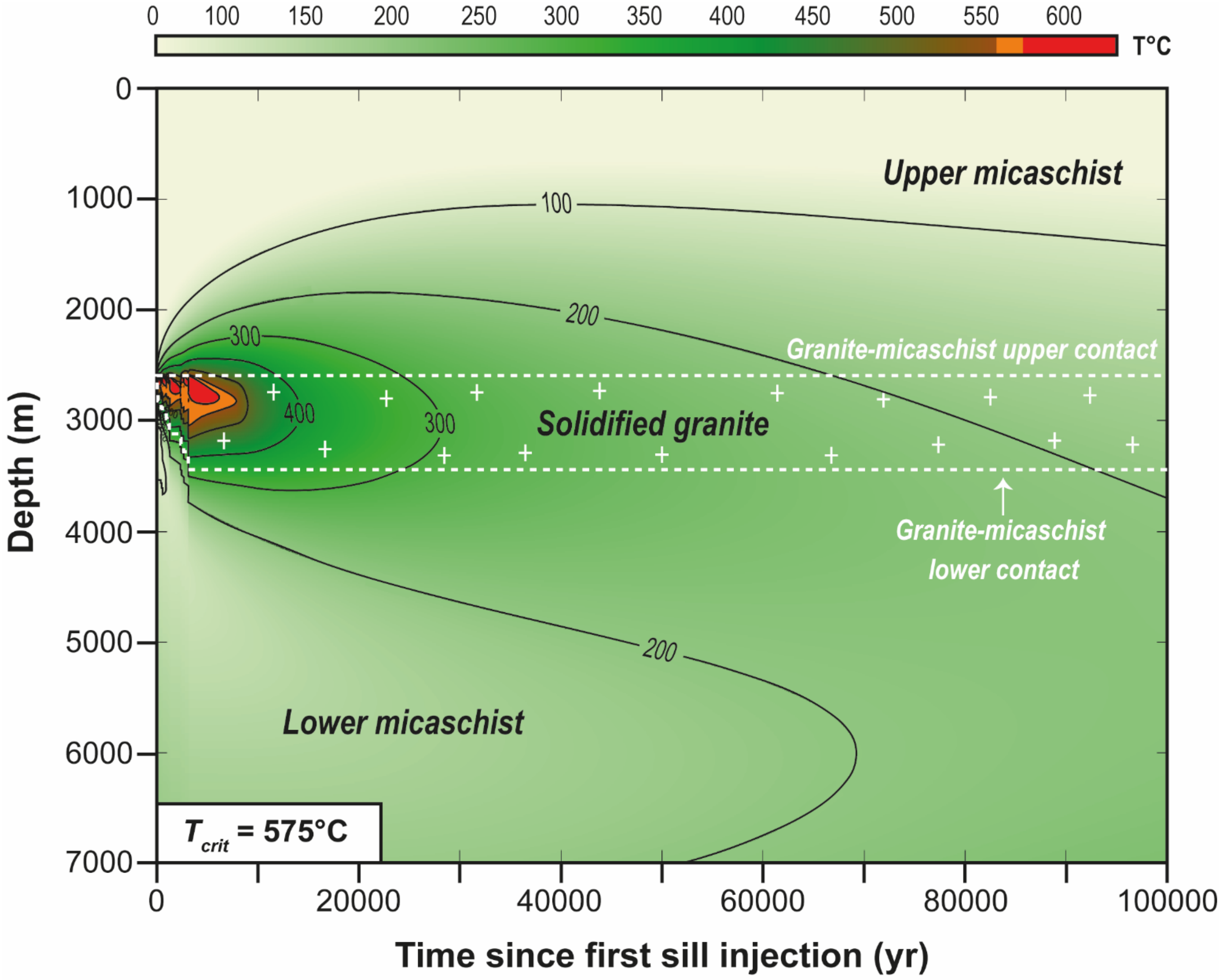

Supplementary figure A5: Assembly and lifetime durations of the BG as function of T_{crit} for different values of (a) the geothermal gradient (∇T), (b) the specific heat (c), and (c) the latent heat of crystallisation (L). Thermo-kinectic models were performed using the preferred values of L (i.e. 350,000 J.kg^{-1}) and c (i.e. 1,090 J.kg^{-1}.°C^{-1}) in (a), that of ∇T (i.e. 30 °C.km^{-1}) and L in (b), and that of ∇T and c in (c) to see the individual effect of ∇T, c and L, respectively. In (a), note that the variation of ∇T from 20 to 40 °C.km^{-1} (or 60 to 120 °C at 3 km depth) does not significantly affect the lifespan of the BG. In (b), note that the variation of c from 900 to 1500 J.kg^{-1}.°C does not significantly affect the lifespan of the BG. In (c), note that the variation of L from 250,000 to 450,000 J.kg^{-1} affect the lifespan of the BG by a factor ~2, although the durations stay in the same order of magnitude. Also note that regardless the choosen value for ∇T, c and L, the minimum lifespan of the BG is obtained when the assembly duration become longer than the solidification duration after the emplacement of the last sill.

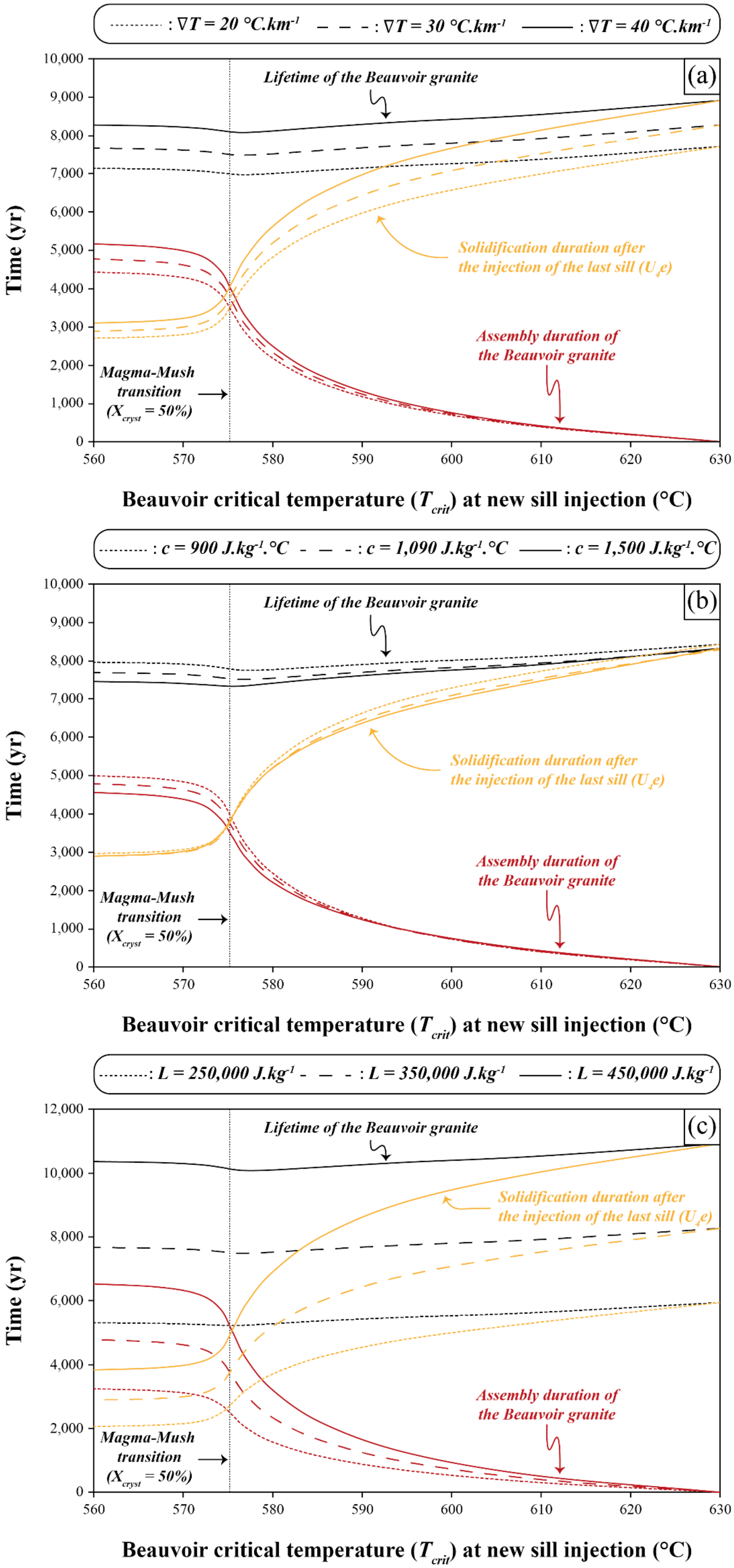

: ∇T = 20 °C.km-1
: ∇T = 30 °C.km-1
: ∇T = 40 °C.km-1
(a)
Lifetime of the Beauvoir granite
Solidification duration after the injection of the last sill (U4e)
Assembly duration of the Beauvoir granite
Magma-Mush transition (Xcryst = 50%)
Time (yr)
Beauvoir critical temperature (Tcrit) at new sill injection (°C)
: c = 900 J.kg-1.°C
: c = 1,090 J.kg-1.°C
: c = 1,500 J.kg-1.°C
(b)
Lifetime of the Beauvoir granite
Solidification duration after the injection of the last sill (U4e)
Assembly duration of the Beauvoir granite
Magma-Mush transition (Xcryst = 50%)
Time (yr)
Beauvoir critical temperature (Tcrit) at new sill injection (°C)
: L = 250,000 J.kg-1
: L = 350,000 J.kg-1
: L = 450,000 J.kg-1
(c)
Lifetime of the Beauvoir granite
Solidification duration after the injection of the last sill (U4e)
Assembly duration of the Beauvoir granite
Magma-Mush transition (Xcryst = 50%)
Time (yr)
Beauvoir critical temperature (Tcrit) at new sill injection (°C)

Supplementary figure A6: Compilation of inferred average pluton construction rates based on their construction durations and their estimated volume (adapted from *de Saint Blanquat et al. 2011*). (a) Plutons distinction based on their tectonic setting, and (b) pluton distinction based on their global chemistry. List of plutons references: 1 - Beauvoir granite (this study); 2 – Sant'Andrea (Barboni et Schoene 2014); 3 – Monte Capanne (Barboni et al. 2015); 4 – Corno Alto (Schaltegger et al. 2019); 5 – Val Freda (Broderick et al. 2015); 6 – Lago della Vacca (Schoene et al. 2012); 7 – North Re di Castello (Schaltegger et al. 2019); 8 - Western Adamello Tonalite (Schaltegger et al. 2019); 9 - Avio (Schaltegger et al. 2019); 10 – Presanella (Schaltegger et al. 2019); 11 – Bergell (Samperton et al. 2015); 12 – Saint-Jean-du-Doigt (Barboni et al. 2013); 13 – Tinos (de Saint Blanquat et al. 2001; Lamont et al. 2023); 14 – PX1 – Pajara (Allibon et al. 2011); 15 – Skaergaard (Annen et al. 2022); 16 – Korosten (Amelin et al. 1994); 17 – Wiborg (Vaasjoki, Tapani Rämö, et Sakko 1991); 18 – Salmi phase 3 (Amelin, Larin, et Tucker 1997); 19 - Manaslu (Annen et al. 2006); 20 – Bushveld (Zeh et al. 2015); 21 – Emerald Lake (Coulson et al. 2002); 22 – Huemul (Schaen et al. 2021); 23 – San Rafael (Markovic et al. 2025); 24 – Torres del Paine (Leuthold et al. 2012); 25 – Black Mesa (de Saint Blanquat et al. 2006); 26 – Mount Stuart (Matzel, Bowring, et Miller 2006); 27 - Tenpeak (Matzel et al. 2006); 28 - Golden Horn Total (Eddy et al. 2016); 29 - Peralkaline granite – Golden Horn (Eddy et al. 2016); 30 - Hypersolvus granite – Golden Horn (Eddy et al. 2016); 31 - Rapakivi granite – Golden Horn (Eddy et al. 2016); 32 - Heterogeneous granite – Golden Horn (Eddy et al. 2016); 33 – Questa (Gaynor, Rosera, et Coleman 2019); 34 – Socorro Magma Body (Fialko et Simons 2001); 35 – Rio Hondo (Tappa et al. 2011); 36 – Papoose Flat (de Saint Blanquat et al. 2011); 37 – Tuolumne Intrusive Suite Total (Coleman, Gray, et Glazner 2004); 38 – Cathedral Peak (Coleman et al. 2004); 39 – Kuna Crest (Coleman et al. 2004); 40 – Half Dome (Coleman et al. 2004); 41 – Mono Creek (de Saint Blanquat et al. 2011); 42 – Lamarck (Davis et al. 2012); 43 – Miur (Davis et al. 2012); 44 – Mount Givens (Frazer, Coleman, et Mills 2014); 45 – Yerington (Schöpa et al. 2017); 46 – Mount Princeton (Mills et Coleman 2013); 47 – San Juan (Lipman et Bachmann 2015); 48 – Spirit Mountain (Walker et al. 2007); 49 – Geyser-Cobb Mountain (Schmitt et al. 2003); 50 – Bingham Canyon (Large et al. 2021); 51 – Scuzzi (Brown et McClelland 2000); 52 – Long term Uturuncu volcano (Sparks et al. 2008); 53 – Bishop Tuff (Chamberlain et al. 2014); 54 – Altiplano-Puna Volcanic Complex (de Silva et Gosnold 2007); 55 – Southern Rocky Mountain Volcanic Field (Lipman 2007); 56 – Karoo Large Igneous Province (Svensen et al. 2012); 57- Oruanui volcano reservoir (Allan et al. 2017); 58 - Yellowstone volcano WYF & PPF reservoirs (Stelten et al. 2015); 59 – Kos Plateau Tuff Reservoir (Bachmann, Charlier, et Lowenstern 2007); 60 - Hualca Hualco volcano (Pritchard et Simons 2002); 61 – Unzen volcano (Nakada et Motomura 1999). Field for the Hawaiian-Emperor basaltic chain is from *Shaw (1985)*. Field for spreading ridges has been calculated for a 1 km long ridge segment based on oceanic crust thickness of 3-7 km and spreading rates of 1-15 $cm.yr^{-1}$ (Chen 1992), leading to average construction rates of ~10^{-3} and 10^{-5} $km^3.yr^{-1}$ for fast and slow spreading ridges, respectively.

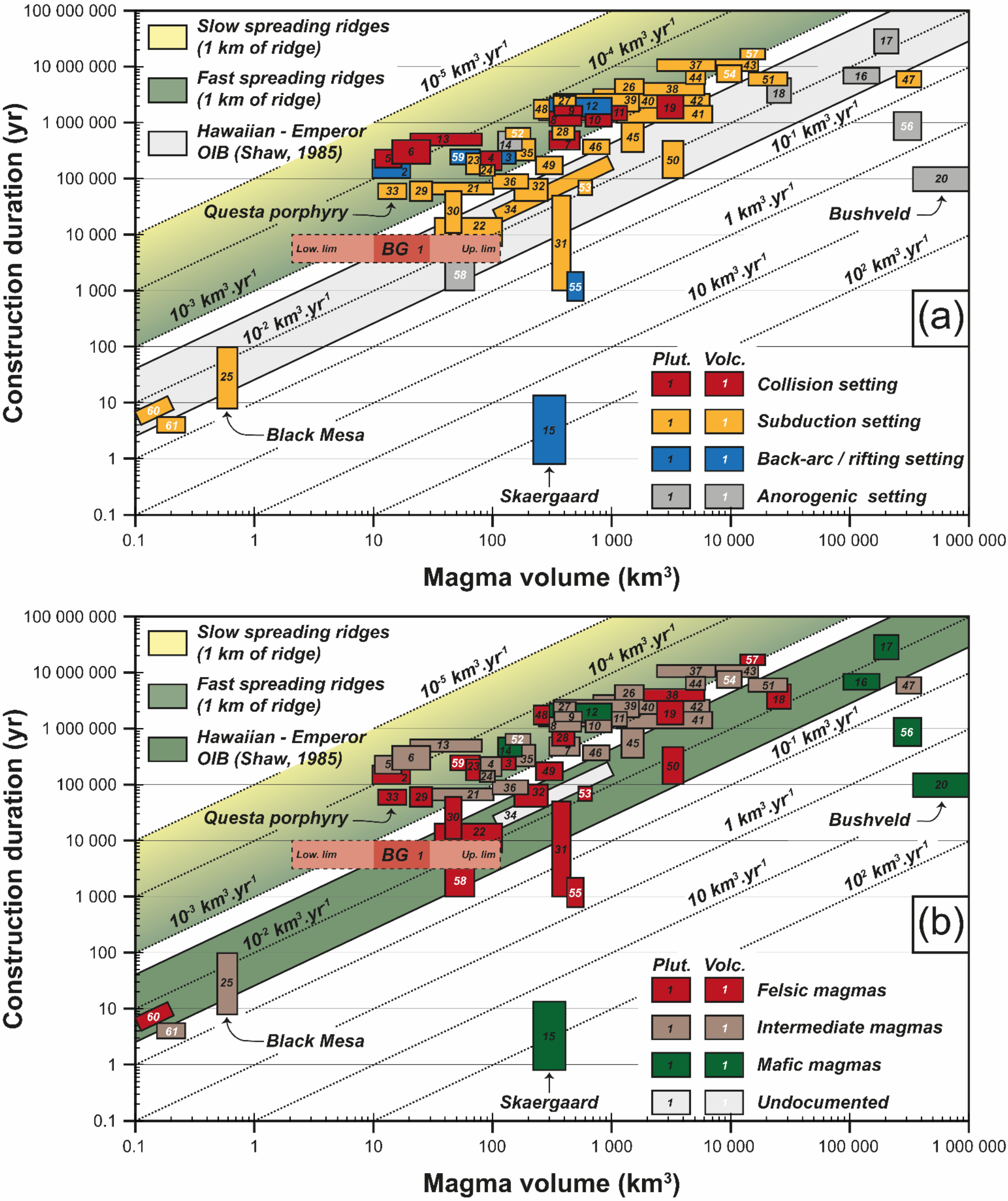

Slow spreading ridges (1 km of ridge)
Fast spreading ridges (1 km of ridge)
Hawaiian - Emperor OIB (Shaw, 1985)
Questa porphyry
Black Mesa
Skaergaard
Bushveld
BG
Low. lim
Up. lim
Construction duration (yr)
Magma volume (km³)
Plut.
Volc.
Collision setting
Subduction setting
Back-arc / rifting setting
Anorogenic setting
(a)
Felsic magmas
Intermediate magmas
Mafic magmas
Undocumented
(b)

Supplementary figure B1: Microphotographs of the investigated biotite-cordierite-sillimanite gneiss from the Bodenmais locality, Germany (a) and from the Namaqualand, South Africa (b-d). Note the overall wide and texturally equilibrated dihedral angles.

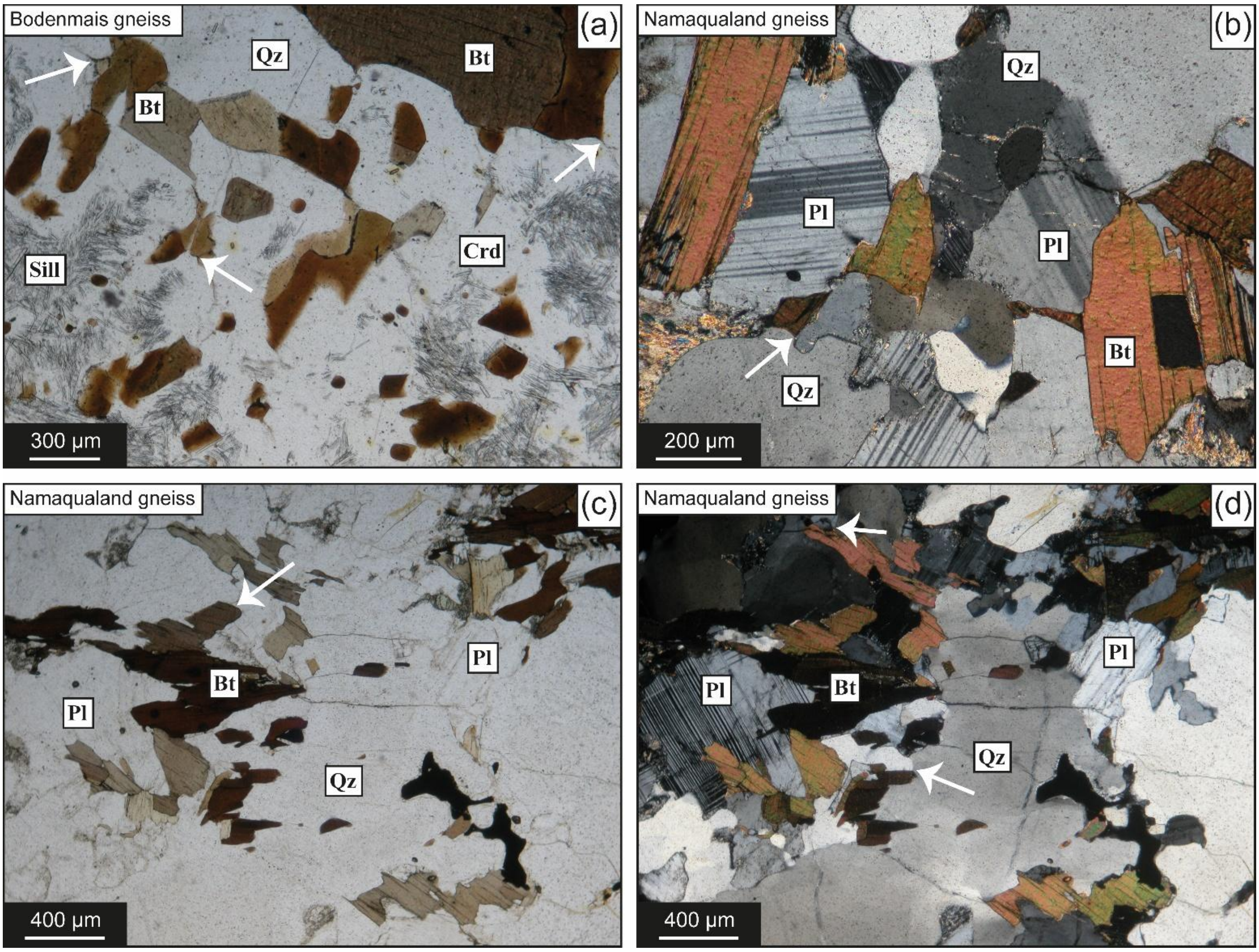

Supplementary figure B2: Cross-polarised microphotographs evidencing partially dissolved plagioclase. (a) 254.23 m (U_4d), (b) 298.78 m (U_4c), (c) 336.35 (U_4b). Note that the plagioclase partial dissolution events were followed by the crystallisation of lepidolite in interstitial position. (d) 672.24 m (U_2c). Note the crystallisation of potassic feldspar within and around the partially dissolved plagioclase.

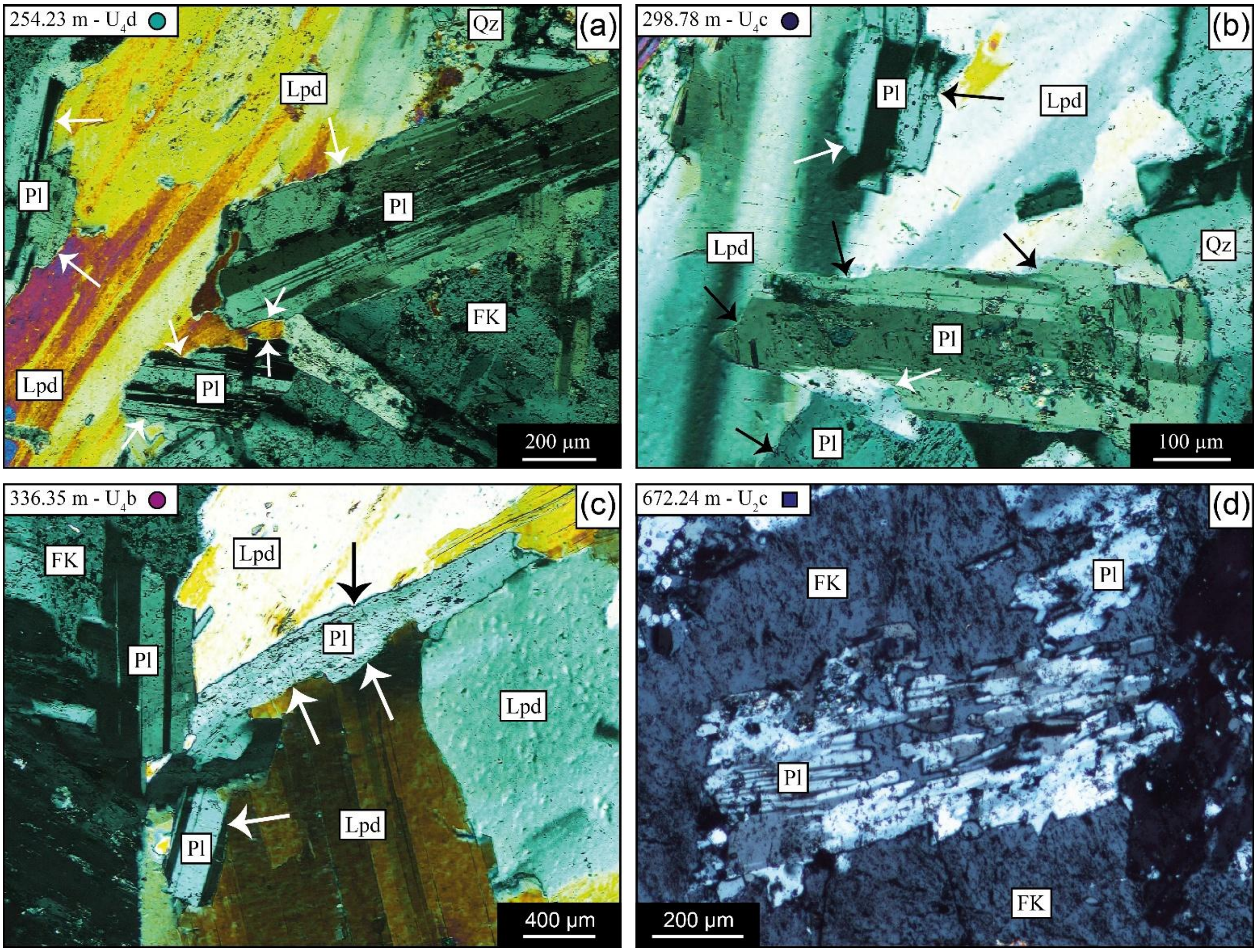

Supplementary Table B1: Measured biotite-plagioclase-plagioclase (Θ_{bpp}) and biotite-quartz-quartz (Θ_{bqq}) dihedral angles (indicated by white arrows) in a cordierite-sillimanite gneiss (Namaqualand, South Africa) and in a cordierite-sillimanite gneiss from the Bodenmais locality (Germany).

Rock type	**Locality**	**n**	**Θ**	**SD**
Cordierite-sillimanite gneiss	Namaqualand	35	Θ_{bpp}: 96 ± 4	9.0
Cordierite-sillimanite gneiss	Bodenmais	35	Θ_{bqq}: 95 ± 2.5	8.0
Cordierite-sillimanite gneiss	Bodenmais	43	Θ_{bqq}: 93 ± 3.5	10.0

Supplementary Table B2: Results of the Chi-2 (χ^2) test performed between each sub-unit pair to see if whether their Θ_{lpp} median values are significantly different. The Z_Value indicates how large the difference between two averages (medium Θ_{lpp} of U_4e and U_4d) is in relation to the combined uncertainties. A Z_Value around 1 will indicate that the difference between the two samples is not significative, while a Z_Value above 3 indicates that this difference is really significative. For instance, the Z_Value of the U_4e-U_4d pair is obtained with the following equation:

$$\boldsymbol{Z}_{[\boldsymbol{U_4}\mathbf{e}-\boldsymbol{U_4}\mathbf{d}]} = \frac{\boldsymbol{\Theta}_{\boldsymbol{U4e}} - \boldsymbol{\Theta}_{\boldsymbol{U4d}}}{\sqrt{\pm\boldsymbol{\Theta}^2_{\boldsymbol{U4e}} + \pm\boldsymbol{\Theta}^2_{\boldsymbol{U4d}}}} \quad (1)$$

with Θ corresponds to the median Θ_{lpp} value of the population, and $\pm\Theta$ to the uncertainty related to the median value (calculated according to *Stickels and Hücke, 1964*).

The P_Value indicates the probability of obtaining a deviation at least as large as that observed if, in reality, the two samples (e.g., U_4e and U_4d) measure the same process. For instance, the P_Value of the U_4e-U_4d pair is obtained with the following equation:

$$\boldsymbol{P}_{[\boldsymbol{U_4}\mathbf{e}-\boldsymbol{U_4}\mathbf{d}]} = \mathbf{2} \times (\mathbf{1} - \boldsymbol{\Phi} \times \boldsymbol{Z}_{[\boldsymbol{U_4}\mathbf{e}-\boldsymbol{U_4}\mathbf{d}]}) \quad (2)$$

with $\boldsymbol{\Phi}$ is the distribution function of the standard normal distribution. A P_Value > 0.05 indicates that there is no significative difference between the two tested samples. A P_Value < 0.05 indicates there is a significative statistically difference between the two tested samples, while a P_Value < 0.01 indicates that this difference is really significant.

Sub-unit pair	Θ_{lpp} difference	Z_Value	P_value	Significative?
U_4e-U_4d	8	0.94	0.34578	No
U_4e-U_4b	4	0.53	0.59380	No
U_4e-U_4a	4	0.58	0.56471	No
U_4e-U_3b	2.5	0.25	0.80259	No
U_4e-U_3a	6	0.60	0.54851	No
U_4e-U_2i	2.5	0.24	0.81011	No
U_4e-U_2g	7.5	0.78	0.43488	No
U_4e-U_2f	2	0.25	0.80590	No
U_4e-U_2e	7	0.93	0.35065	No
U_4e-U_2d	1	0.09	0.92634	No
U_4e-U_2a	4	0.37	0.71153	No
U_4d-U_4b	4	0.53	0.59380	No
U_4d-U_4a	12	1.73	0.08407	No
U_4d-U_3b	10.5	1.05	0.29372	No
U_4d-U_3a	14	1.40	0.16151	No
U_4d-U_2i	10.5	1.01	0.31288	No
U_4d-U_2g	15.5	1.61	0.10657	No
U_4d-U_2f	6	0.74	0.46103	No
U_4d-U_2e	15	2.00	0.04550	Yes
U_4d-U_2d	9	0.83	0.40538	No
U_4d-U_2a	12	1.11	0.26726	No
U_4b-U_4a	8	1.40	0.16053	No
U_4b-U_3b	6.5	0.71	0.47885	No
U_4b-U_3a	10	1.09	0.27595	No

U_4b-U_2i	6.5	0.68	0.49914	No
U_4b-U_2g	11.5	1.31	0.18857	No
U_4b-U_2f	2	0.28	0.77837	No
U_4b-U_2e	11	1.73	0.08390	No
U_4b-U_2d	5	0.50	0.61926	No
U_4b-U_2a	8	0.80	0.42659	No
U_4a-U_3b	1.5	0.17	0.86361	No
U_4a-U_3a	2	0.23	0.81884	No
U_4a-U_2i	1.5	0.16	0.87038	No
U_4a-U_2g	3.5	0.42	0.67238	No
U_4a-U_2f	6	0.92	0.35739	No
U_4a-U_2e	3	0.53	0.59873	No
U_4a-U_2d	3	0.31	0.75605	No
U_4a-U_2a	0	0.00	1.00000	No
U_3b-U_3a	3.5	0.31	0.75705	No
U_3b-U_2i	0	0.00	1.00000	No
U_3b-U_2g	5	0.46	0.64842	No
U_3b-U_2f	4.5	0.46	0.64299	No
U_3b-U_2e	4.5	0.49	0.62395	No
U_3b-U_2d	1.5	0.12	0.90087	No
U_3b-U_2a	1.5	0.12	0.90087	No
U_3a-U_2i	3.5	0.30	0.76429	No
U_3a-U_2g	1.5	0.14	0.89120	No
U_3a-U_2f	8	0.82	0.40992	No
U_3a-U_2e	1	0.11	0.91324	No
U_3a-U_2d	5	0.42	0.67798	No
U_3a-U_2a	2	0.17	0.86809	No
U_2i-U_2g	5	0.44	0.65915	No
U_2i-U_2f	4.5	0.44	0.65670	No
U_2i-U_2e	4.5	0.47	0.63986	No
U_2i-U_2d	1.5	0.12	0.90356	No
U_2i-U_2a	1.5	0.12	0.90356	No
U_2g-U_2f	9.5	1.02	0.30704	No
U_2g-U_2e	0.5	0.06	0.95441	No
U_2g-U_2d	6.5	0.55	0.57901	No
U_2g-U_2a	3.5	0.30	0.76513	No
U_2f-U_2e	9	1.27	0.20534	No
U_2f-U_2d	3	0.28	0.77608	No
U_2f-U_2a	6	0.57	0.56945	No
U_2e-U_2d	6	0.60	0.55098	No
U_2e-U_2a	3	0.30	0.76559	No
U_2d-U_2a	3	0.24	0.81366	No

References:

Allan, Aidan. S. R., Simon J. Barker, Marc-Alban Millet, Daniel J. Morgan, Shane M. Rooyakkers, C. Ian Schipper, et Colin J. N. Wilson. 2017. « A Cascade of Magmatic Events during the Assembly and Eruption of a Super-Sized Magma Body ». *Contributions to Mineralogy and Petrology* 172(7):49. doi:10.1007/s00410-017-1367-8.

Allibon, J., F. Bussy, É. Lewin, et B. Darbellay. 2011. « The Tectonically Controlled Emplacement of a Vertically Sheeted Gabbro-Pyroxenite Intrusion: Feeder-Zone of an Ocean-Island Volcano (Fuerteventura, Canary Islands) ». *Tectonophysics* 500(1-4):78-97. doi:10.1016/j.tecto.2010.01.011.

Amelin, Y. V., Anatoly M. Larin, et Robert D. Tucker. 1997. « Chronology of Multiphase Emplacement of the Salmi Rapakivi Granite-Anorthosite Complex, Baltic Shield: Implications for Magmatic Evolution ». *Contributions to Mineralogy and Petrology* 127(4):353-68. doi:10.1007/s004100050285.

Amelin, Yu. V., L. M. Heaman, V. M. Verchogliad, et V. M. Skobelev. 1994. « Geochronological Constraints on the Emplacement History of an Anorthosite ? Rapakivi Granite Suite: U?Pb Zircon and Baddeleyite Study of the Korosten Complex, Ukraine ». *Contributions to Mineralogy and Petrology* 116(4):411-19. doi:10.1007/BF00310908.

Annen, C., B. Scaillet, et R. S. J. Sparks. 2006. « Thermal Constraints on the Emplacement Rate of a Large Intrusive Complex: The Manaslu Leucogranite, Nepal Himalaya ». *Journal of Petrology* 47(1):71-95. doi:10.1093/petrology/egi068.

Annen, Catherine, Rais Latypov, Sofya Chistyakova, Alexander R. Cruden, et Troels F. D. Nielsen. 2022. « Catastrophic Growth of Totally Molten Magma Chambers in Months to Years ». *Science Advances* 8(38):eabq0394. doi:10.1126/sciadv.abq0394.

Bachmann, O., B. L. A. Charlier, et J. B. Lowenstern. 2007. « Zircon Crystallization and Recycling in the Magma Chamber of the Rhyolitic Kos Plateau Tuff (Aegean Arc) ». *Geology* 35(1):73. doi:10.1130/G23151A.1.

Barboni, Mélanie, Catherine Annen, et Blair Schoene. 2015. « Evaluating the Construction and Evolution of Upper Crustal Magma Reservoirs with Coupled U/Pb Zircon Geochronology and Thermal Modeling: A Case Study from the Mt. Capanne Pluton (Elba, Italy) ». *Earth and Planetary Science Letters* 432:436-48. doi:10.1016/j.epsl.2015.09.043.

Barboni, Mélanie, et Blair Schoene. 2014. « Short Eruption Window Revealed by Absolute Crystal Growth Rates in a Granitic Magma ». *Nature Geoscience* 7(7):524-28. doi:10.1038/ngeo2185.

Barboni, Mélanie, Blair Schoene, Maria Ovtcharova, François Bussy, Urs Schaltegger, et Axel Gerdes. 2013. « Timing of Incremental Pluton Construction and Magmatic Activity in a Back-Arc Setting Revealed by ID-TIMS U/Pb and Hf Isotopes on Complex Zircon Grains ». *Chemical Geology* 342:76-93. doi:10.1016/j.chemgeo.2012.12.011.

Bohrson, W. A., et Frank J. Spera. 2001. « Energy-Constrained Open-System Magmatic Processes II: Application of Energy-Constrained Assimilation-Fractional Crystallization (EC-AFC) Model to Magmatic Systems ». *Journal of Petrology* 42(5):1019-41. doi:10.1093/petrology/42.5.1019.

Broderick, C., J. F. Wotzlaw, D. A. Frick, A. Gerdes, A. Ulianov, D. Günther, et U. Schaltegger. 2015. « Linking the Thermal Evolution and Emplacement History of an Upper-Crustal Pluton to Its Lower-Crustal Roots Using Zircon Geochronology and Geochemistry (Southern Adamello Batholith, N. Italy) ». *Contributions to Mineralogy and Petrology* 170(3):28. doi:10.1007/s00410-015-1184-x.

Brown, E. H., et W. C. McClelland. 2000. « Pluton Emplacement by Sheeting and Vertical Ballooning in Part of the Southeast Coast Plutonic Complex, British Columbia ». *Geological Society of America Bulletin* 112(5):708-19. doi:https://doi.org/10.1130/0016-7606(2000)112<708:PEBSAV>2.0.CO;2.

Chamberlain, K. J., C. J. N. Wilson, J. L. Wooden, B. L. A. Charlier, et T. R. Ireland. 2014. « New Perspectives on the Bishop Tuff from Zircon Textures, Ages and Trace Elements ». *Journal of Petrology* 55(2):395-426. doi:10.1093/petrology/egt072.

Chen, Yongshun John. 1992. « Oceanic crustal thickness versus spreading rate ». *Geophysical Research Letters* 19(8):753-56. doi:https://doi.org/10.1029/92GL00161.

Coleman, Drew S., Walt Gray, et Allen F. Glazner. 2004. « Rethinking the Emplacement and Evolution of Zoned Plutons: Geochronologic Evidence for Incremental Assembly of the Tuolumne Intrusive Suite, California ». *Geology* 32(5):433. doi:10.1130/G20220.1.

Coulson, Ian M., Mike E. Villeneuve, Gregory M. Dipple, Robert A. Duncan, James K. Russell, et James K. Mortensen. 2002. « Time-Scales of Assembly and Thermal History of a Composite Felsic Pluton: Constraints from the Emerald Lake Area, Northern Canadian Cordillera, Yukon ». *Journal of Volcanology and Geothermal Research* 114(3-4):331-56. doi:10.1016/S0377-0273(01)00294-3.

Davis, Jesse W., Drew S. Coleman, John T. Gracely, Richard Gaschnig, et Michael Stearns. 2012. « Magma Accumulation Rates and Thermal Histories of Plutons of the Sierra Nevada Batholith, CA ». *Contributions to Mineralogy and Petrology* 163(3):449-65. doi:10.1007/s00410-011-0683-7.

Eddy, Michael P., Samuel A. Bowring, Robert B. Miller, et Jeffrey H. Tepper. 2016. « Rapid Assembly and Crystallization of a Fossil Large-Volume Silicic Magma Chamber ». *Geology* 44(4):331-34. doi:10.1130/G37631.1.

Esteves, Nicolas, Pierre Bouilhol, Michel Cuney, et Lydéric France. 2026. « Small pluton construction through sills stacking, amalgamation and differentiation: Insight from the Beauvoir granite (Massif Central, France) ». *Accepted at Journal of Petrology*. doi:https://doi.org/10.1093/petrology/egag055.

Fialko, Yuri, et Mark Simons. 2001. « Evidence for On-going Inflation of the Socorro Magma Body, New Mexico, from Interferometric Synthetic Aperture Radar Imaging ». *Geophysical Research Letters* 28(18):3549-52. doi:10.1029/2001GL013318.

Frazer, Ryan E., Drew S. Coleman, et Ryan D. Mills. 2014. « Zircon U-Pb Geochronology of the Mount Givens Granodiorite: Implications for the Genesis of Large Volumes of Eruptible Magma ». *Journal of Geophysical Research: Solid Earth* 119(4):2907-24. doi:10.1002/2013JB010716.

Gaynor, Sean P., Joshua M. Rosera, et Drew S. Coleman. 2019. « Intrusive History of the Oligocene Questa Porphyry Molybdenum Deposit, New Mexico ». *Geosphere* 15(2):548-75. doi:10.1130/GES01675.1.

Huber, Christian, Olivier Bachmann, et Michael Manga. 2009. « Homogenization Processes in Silicic Magma Chambers by Stirring and Mushification (Latent Heat Buffering) ». *Earth and Planetary Science Letters* 283(1-4):38-47. doi:10.1016/j.epsl.2009.03.029.

Lamont, Thomas N., Nick M. W. Roberts, Michael P. Searle, Nicholas J. Gardiner, Phillip Gopon, Yu-Te Hsieh, Philip Holdship, et Richard W. White. 2023. « Contemporaneous Crust-Derived I- and S-Type Granite Magmatism and Normal Faulting on Tinos, Delos, and Naxos, Greece: Constraints on Aegean Orogenic Collapse ». *Geological Society of America Bulletin* 135(11/12):2797-2829. doi:https://doi.org/10.1130/B36489.1.

Large, S. J. E., Y. Buret, J. F. Wotzlaw, O. Karakas, M. Guillong, A. Von Quadt, et C. A. Heinrich. 2021. « Copper-Mineralised Porphyries Sample the Evolution of a Large-Volume Silicic Magma Reservoir from Rapid Assembly to Solidification ». *Earth and Planetary Science Letters* 563:116877. doi:10.1016/j.epsl.2021.116877.

Leuthold, Julien, Othmar Müntener, Lukas P. Baumgartner, Benita Putlitz, Maria Ovtcharova, et Urs Schaltegger. 2012. « Time Resolved Construction of a Bimodal Laccolith (Torres Del Paine, Patagonia) ». *Earth and Planetary Science Letters* 325-326:85-92. doi:10.1016/j.epsl.2012.01.032.

Lipman, Peter W. 2007. « Incremental Assembly and Prolonged Consolidation of Cordilleran Magma Chambers: Evidence from the Southern Rocky Mountain Volcanic Field ». *Geosphere* 3(1):42. doi:10.1130/GES00061.1.

Lipman, Peter W., et Olivier Bachmann. 2015. « Ignimbrites to Batholiths: Integrating Perspectives from Geological, Geophysical, and Geochronological Data ». *Geosphere* 11(3):705-43. doi:10.1130/GES01091.1.

Markovic, Sava, Dawid Szymanowski, Lorenzo Tavazzani, Lisard Torró, Kalin Kouzmanov, Miroslav Kalinaj, et Cyril Chelle-Michou. 2025. « Timescales of Magmatic-Hydrothermal Activity at the Giant San Rafael Tin Deposit (Peru) ». *Earth and Planetary Science Letters* 671:119624. doi:10.1016/j.epsl.2025.119624.

Matzel, J. E. P., S. A. Bowring, et R. B. Miller. 2006. « Time Scales of Pluton Construction at Differing Crustal Levels: Examples from the Mount Stuart and Tenpeak Intrusions, North Cascades, Washington ». *Geological Society of America Bulletin* 118(11-12):1412-30. doi:10.1130/B25923.1.

Mills, Ryan D., et Drew S. Coleman. 2013. « Temporal and Chemical Connections between Plutons and Ignimbrites from the Mount Princeton Magmatic Center ». *Contributions to Mineralogy and Petrology* 165(5):961-80. doi:10.1007/s00410-012-0843-4.

Nakada, Setsuya, et Yoshinobu Motomura. 1999. « Petrology of the 1991–1995 Eruption at Unzen: Effusion Pulsation and Groundmass Crystallization ». *Journal of Volcanology and Geothermal Research* 89(1-4):173-96. doi:10.1016/S0377-0273(98)00131-0.

Pritchard, Matthew E., et Mark Simons. 2002. « A Satellite Geodetic Survey of Large-Scale Deformation of Volcanic Centres in the Central Andes ». *Nature* 418(6894):167-71. doi:10.1038/nature00872.

Robertson, Eugene C. 1988. *Thermal Properties of Rocks*. United State Departement of the Interior Geological Survey.

de Saint Blanquat, Michel, Guillaume Habert, Eric Horsman, Sven S. Morgan, Basil Tikoff, Patrick Launeau, et Gérard Gleizes. 2006. « Mechanisms and Duration of Non-Tectonically Assisted Magma Emplacement in the Upper Crust: The Black Mesa Pluton, Henry Mountains, Utah ». *Tectonophysics* 428(1-4):1-31. doi:10.1016/j.tecto.2006.07.014.

de Saint Blanquat, Michel, Eric Horsman, Guillaume Habert, Sven Morgan, Olivier Vanderhaeghe, Richard Law, et Basil Tikoff. 2011. « Multiscale Magmatic Cyclicity, Duration of Pluton Construction, and the Paradoxical Relationship between Tectonism and Plutonism in Continental Arcs ». *Tectonophysics* 500(1-4):20-33. doi:10.1016/j.tecto.2009.12.009.

de Saint Blanquat, Michel, Richard D. Law, Jean-Luc Bouchez, et Sven S. Morgan. 2001. « Internal Structure and Emplacement of the Papoose Flat Pluton: An Integrated Structural, Petrographic, and Magnetic Susceptibility Study ». *Geological Society of America Bulletin* 113(8):976-95. doi:10.1130/0016-7606(2001)113<0976:ISAEOT>2.0.CO;2.

Samperton, Kyle M., Blair Schoene, John M. Cottle, C. Brenhin Keller, James L. Crowley, et Mark D. Schmitz. 2015. « Magma Emplacement, Differentiation and Cooling in the Middle Crust: Integrated Zircon Geochronological–Geochemical Constraints from the Bergell Intrusion, Central Alps ». *Chemical Geology* 417:322-40. doi:10.1016/j.chemgeo.2015.10.024.

Schaen, Allen J., Blair Schoene, Josef Dufek, Brad S. Singer, Michael P. Eddy, Brian R. Jicha, et John M. Cottle. 2021. « Transient Rhyolite Melt Extraction to Produce a Shallow Granitic Pluton ». *Science Advances* 7(21):eabf0604. doi:10.1126/sciadv.abf0604.

Schaltegger, U., A. Nowak, A. Ulianov, C. M. Fisher, A. Gerdes, R. Spikings, M. J. Whitehouse, I. Bindeman, J. M. Hanchar, J. Duff, J. D. Vervoort, T. Sheldrake, L. Caricchi, P. Brack, et O. Müntener. 2019. « Zircon Petrochronology and 40Ar/39Ar Thermochronology of the Adamello Intrusive Suite, N. Italy: Monitoring the Growth and Decay of an Incrementally Assembled Magmatic System ». *Journal of Petrology* 60(4):701-22. doi:10.1093/petrology/egz010.

Schmitt, Axel K., Marty Grove, T. Mark Harrison, Oscar Lovera, Jeffrey Hulen, et Mark Walters. 2003. « The Geysers-Cobb Mountain Magma System, California (Part 2): Timescales of Pluton Emplacement and Implications for Its Thermal History ». *Geochimica et Cosmochimica Acta* 67(18):3443-58. doi:10.1016/S0016-7037(03)00126-1.

Schoene, Blair, Urs Schaltegger, Peter Brack, Christopher Latkoczy, Andreas Stracke, et Detlef Günther. 2012. « Rates of Magma Differentiation and Emplacement in a Ballooning Pluton Recorded by U–Pb TIMS-TEA, Adamello Batholith, Italy ». *Earth and Planetary Science Letters* 355-356:162-73. doi:10.1016/j.epsl.2012.08.019.

Schöpa, Anne, Catherine Annen, John H. Dilles, R. Stephen J. Sparks, et Jon D. Blundy. 2017. « Magma Emplacement Rates and Porphyry Copper Deposits: Thermal Modeling of the Yerington Batholith, Nevada ». *Economic Geology* 112(7):1653-72. doi:10.5382/econgeo.2017.4525.

Shaw, Herbert R. 1985. « Links between Magma-tectonic Rate Balances, Plutonism, and Volcanism ». *Journal of Geophysical Research: Solid Earth* 90(B13):11275-88. doi:10.1029/JB090iB13p11275.

de Silva, Shanaka L., et William D. Gosnold. 2007. « Episodic Construction of Batholiths: Insights from the Spatiotemporal Development of an Ignimbrite Flare-Up ». *Journal of Volcanology and Geothermal Research* 167(1-4):320-35. doi:10.1016/j.jvolgeores.2007.07.015.

Sparks, R. S. J., C. B. Folkes, M. C. S. Humphreys, D. N. Barfod, J. Clavero, M. C. Sunagua, S. R. McNutt, et M. E. Pritchard. 2008. « Uturuncu Volcano, Bolivia: Volcanic Unrest Due to Mid-Crustal Magma Intrusion ». *American Journal of Science* 308(6):727-69. doi:10.2475/06.2008.01.

Stelten, Mark E., Kari M. Cooper, Jorge A. Vazquez, Andrew T. Calvert, et Justin J. G. Glessner. 2015. « Mechanisms and Timescales of Generating Eruptible Rhyolitic Magmas at Yellowstone Caldera from Zircon and Sanidine Geochronology and Geochemistry ». *Journal of Petrology* 56(8):1607-42. doi:10.1093/petrology/egv047.

Stickels, Ch A., et EE Hücke. 1964. « Measurement of dihedral angles ». *Transactions of the Metallurgical Society of AIME* 230(4):795.

Svensen, Henrik, Fernando Corfu, Stéphane Polteau, Øyvind Hammer, et Sverre Planke. 2012. « Rapid Magma Emplacement in the Karoo Large Igneous Province ». *Earth and Planetary Science Letters* 325-326:1-9. doi:10.1016/j.epsl.2012.01.015.

Tappa, Michael J., Drew S. Coleman, Ryan D. Mills, et Kyle M. Samperton. 2011. « The Plutonic Record of a Silicic Ignimbrite from the Latir Volcanic Field, New Mexico: PLUTON-IGNIMBRITE CONNECTIONS, QUESTA, NM ». *Geochemistry, Geophysics, Geosystems* 12(10):n/a-n/a. doi:10.1029/2011GC003700.

Vaasjoki, Matti, O. Tapani Rämö, et Matti Sakko. 1991. « New U-Pb Ages from the Wiborg Rapakivi Area: Constraints on the Temporal Evolution of the Rapakivi Granite-Anorthosite-Diabase Dyke Association of Southeastern Finland ». *Precambrian Research* 51(1-4):227-43. doi:10.1016/0301-9268(91)90102-G.

Walker, B. A., C. F. Miller, L. Lowery Claiborne, J. L. Wooden, et J. S. Miller. 2007. « Geology and Geochronology of the Spirit Mountain Batholith, Southern Nevada: Implications for Timescales and Physical Processes of Batholith Construction ». *Journal of Volcanology and Geothermal Research* 167(1-4):239-62. doi:10.1016/j.jvolgeores.2006.12.008.

Zeh, Armin, Maria Ovtcharova, Allan H. Wilson, et Urs Schaltegger. 2015. « The Bushveld Complex was emplaced and cooled in less than one million years–results of zirconology, and geotectonic implications ». *Earth and Planetary Science Letters* 418:103-14. doi:https://doi.org/10.1016/j.epsl.2015.02.035.